Stabilization of Cu^{III} under High Pressure in Sr_2CuGaO_5

M. L. Ruiz-González,[†] C. Prieto,[‡] J. Alonso,[‡] J. Ramírez-Castellanos,[†] and J. M. González-Calbet*,[†]

Departamento de Química Inorgánica, Facultad de Ciencias Químicas, Universidad Complutense de Madrid, E28040 Madrid, Spain, and Instituto de Ciencia de Materiales de Madrid, CSIC, Cantoblanco, 28049 Madrid, Spain

Received July 20, 2001. Revised Manuscript Received January 25, 2002

High pressure has been shown to be a powerful tool to isolate a new compound with Cu^{III}: Sr_2CuGaO_5, the $n = 1$ term of the homologous series $GaSr_2Ca_{n-1}Cu_nO_{2n+3}$. The structural characterization, performed by means of X-ray diffraction, selected area electron diffraction, high-resolution electron microscopy, and X-ray absorption spectroscopy, suggests a related brownmillerite structure, involving a superstructure along the *b* axis and disorder along the *a* axis. Those facts have been explained on the basis of the presence of two kinds of tetrahedral chains. The chemical composition as determined by energy-dispersive X-ray spectroscopy and thermogravimetric analysis confirms the stabilization of Cu as Cu^{III}. Susceptibility measurements show a paramagnetic behavior in agreement with the absence of 2D CuO_2 planes.

Introduction

In the last two decades many oxygen-deficient perovskite-related compounds have been studied, leading to a better understanding of the ways that solids accommodate compositional variations. A well-known perovskite-related structure is the brownmillerite, $A_2B_2O_5$, built up from the ordered intergrowth between corner-sharing [BO_6] octahedral and [BO_4] tetrahedral layers. The orientation of the tetrahedral chains in consecutive layers, i.e., at $y = 1/4$ and $y = 3/4$, is different, since they are related by a 2-fold axis in brownmillerite itself, $Ca_2(Fe,Al)_2O_5$[1] (space group *Ibm*2) and by $\bar{1}$ in $Ca_2Fe_2O_5$[2] (space group *Pcmn*).

Intermediate phases between perovskite and brownmillerite structures have been reported in several oxygen-deficient systems.[3−5] Since the discovery of high-T_c superconductivity in the La−Ba−Cu−O system, this kind of study was widely extended to copper mixed oxides, suggesting that the presence of 2D CuO_2 planes as well as a mixture of Cu^{II} and Cu^{III} oxidation states seems to be necessary to obtain p-type superconductivity in this system. An interesting example which combines the CuO_2 planes with related brownmillerite blocks is the high-pressure homologous series $GaSr_2Ca_{n-1}Cu_nO_{2n+3}$.[6,7] Such a series can be described on the basis of ordered intergrowths between P−T−P (P = pyramid, T = tetrahedron) and IL (infinite layer), i.e., CuO_4 square planes sharing corners. The $n = 2$ term is built up of P−T−P blocks. Higher terms incorporate half an IL unit cell ($n = 3$), i.e., a layer of CuO_2 planes exhibiting $T_c = 70$ K, and one IL unit cell ($n = 4$), i.e., two layers of CuO_2 planes showing a higher T_c, 107 K. Both terms involve Cu^{II} and Cu^{III} oxidation states. Although the $n = 1$ term has not been reported up to now, a brownmillerite structure has been predicted.[7] A schematic representation of such models is depicted in Figure 1. It is worth mentioning that in such $n = 1$ term loss in the 2D copper planes the disappearance of superconductiv-

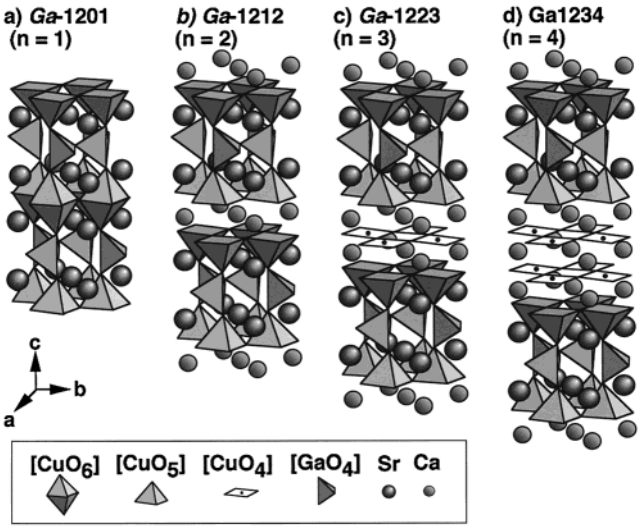

Figure 1. Idealized structural models corresponding to the $n = 1$, 2, 3, and 4 terms of the homologous series $GaSr_2Ca_{n-1}CunO_{2n+3}$.

* To whom correspondence should be addressed. Fax: 34 91 3944342. E-mail: jgcalbet@quim.sim.ucm.es.
[†] Universidad Complutense de Madrid.
[‡] CSIC.

(1) Colville, A.; Séller, S. *Acta Crystallogr.* **1973**, *B27*, 2311.
(2) Bertaut, E. F. *Acta Crystallogr.* **1959**, *12*, 149.
(3) Grenier, J. C.; Darriet, J.; Pouchard, M.; Hagenmuller, P. *Mater. Res. Bull.* **1976**, *11*, 1219.
(4) Hervieu, M.; Nguyen, N.; Caignaert, V.; Raveau, B. *Phys. Status Solidi A* **1984**, *83*, 473.
(5) González-Calbet, J. M.; Vallet-Regí, M. *J. Solid State Chem.* **1987**, *68*, 266.
(6) Isobe, M.; Matsui, Y.; Takayama-Muromachi, E. *Physica C* **1991**, *222*, 310.
(7) Ramírez-Castellanos, J.; Matsui, Y.; Takayama-Muromachi, E.; Isobe, M. *Physica C* **1995**, *251*, 279.

10.1021/cm0111884 CCC: $22.00
Published on Web 04/04/2002

ity is foreseeable. Moreover, this compound would have the "Sr_2CuGaO_5" composition, which should involve all Cu as Cu^{III} instead of a mixed oxidation state. The presence of only Cu^{III} makes the stabilization of this oxide difficult, a higher oxygen pressure being needed to enhance the hole concentration. In this sense, Demazeau et al.[8] reported the high-pressure synthesis of $LaCuO_3$, a rhombohedrally distorted perovskite with Cu^{III}. Superconductivity was not detected in agreement with the above description. A simple way to stabilize the $n = 1$ term is by substituting a 3+ cation such as La^{3+} by Sr^{2+}. In fact, the compounds $LaCaCuGaO_5$,[9] $LaSrCuGaO_5$,[10] and $LaBaCuGaO_5$[11] have been described as showing the brownmillerite structure. In these cases, Cu stabilizes as Cu^{II}, and they are paramagnetic.

Here, we report the high-pressure synthesis and structural characterization of the $n = 1$ term, Sr_2CuGaO_5, corresponding to the $GaSr_2Ca_{n-1}Cu_nO_{2n+3}$ homologous series, which, in fact, is a new compound with all Cu^{III}. Although a brownmillerite structure was expected and preliminary results are in agreement with the previously proposed model,[7] order−disorder phenomena involving tetrahedral chains have been observed.

Experimental Section

A stoichiometric mixture of $SrCO_3$, Ga_2O_3, and CuO, previously decarbonated, was used as the starting material for the high-pressure synthesis of Sr_2CuGaO_5. This powder was sealed in a cylindrical gold capsule, being pressed under 6 GPa at 1000 °C for $^1/_2$ h in a conventional cubic-anvil-type apparatus. The temperature was monitored with a Pt−PtRh thermocouple placed near the gold capsule. $KClO_4$ was added at both the bottom and top of the capsule as an oxygen source. Two very thin gold foils were put between the sample and the $KClO_4$ to avoid sample contamination, but with a small hole in the middle to allow oxygen flux.

Analysis of the chemical composition was carried out by energy-dispersive X-ray spectroscopy (EDS) using a JEOL 2000 FX microscope equipped with a LINK AN10000EXL microanalytical system. Powder X-ray diffraction (XRD) was performed using a Philips X'Pert diffractometer with Cu Kα radiation. The oxygen content, and then the oxidation state of Cu, was determined by thermogravimetric analysis using a Cahn D-200 electrobalance equipped with a furnace and a two-channel register, allowing simultaneous recording of the weight loss and the reaction temperature. The oxygen content can be determined within $\pm 5 \times 10^{-3}$ for a sample of total mass of about 5 mg. The sample was reduced by a mixture of H_2 (300 mbar) and He (200 mbar). X-ray absorption experiments were carried out at the XAS-13 beamline at the DCI storage ring (Orsay) with an electron beam energy of 1.85 GeV and an average current of 250 mA. Data were collected by using a fixed exit monochromator with two flat Si (111) crystals; detection was made by using two ion chambers with air fill gas. Selected area diffraction (SAED) and high-resolution electron microscopy (HREM) were carried out on both JEOL 2000-FX and JEOL 4000-EX microscopes. Magnetic susceptibility measurements, in the range of 5−300 K and in a 100 Oe applied field, were made with a SQUID MPMS-XL magnetometer.

(8) Demazeau, G.; Parent, C.; Pouchard, M.; Hagenmuller, P. *Mater. Res. Bull.* **1972**, *7*, 913.
(9) Luzikova, A. V.; Kharlanov, A. L.; Antipov, E. V. *Z. Anorg. Allg. Chem.* **1994**, *620*, 326.
(10) Vaughey, J. T.; Wiley, J. B.; Poeppelmeier, K. R. *Z. Anorg. Allg. Chem.* **1991**, *598*, 327.
(11) Ruiz-González, M. L.; Ramírez-Castellanos, J.; González-Calbet, J. M. *J. Solid State Chem.* **2000**, *155*, 372.

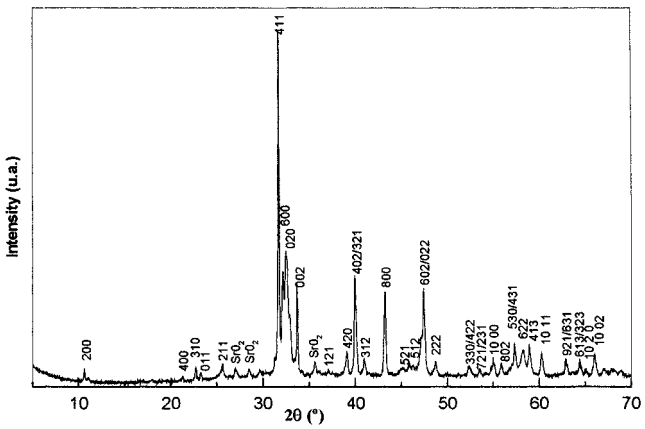

Figure 2. X-ray diffraction pattern marked.

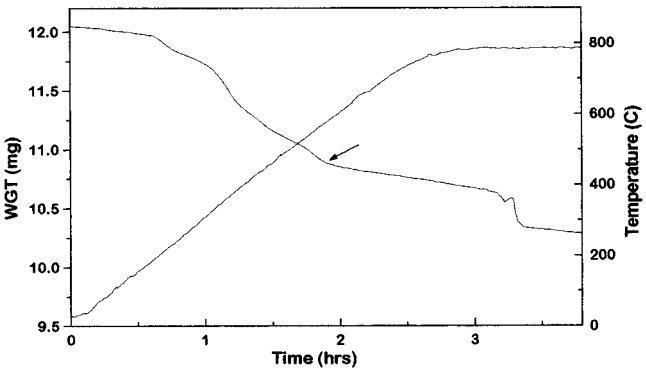

Figure 3. Reduction curve corresponding to Sr_2CuGaO_5. A small plateau is observed at around 450 °C, where $Sr_3Ga_2O_6$ is stabilized, according to XRD data, together with SrO and Cu.

Results and Discussion

The XRD pattern (Figure 2) can be indexed on the basis of a brownmillerite unit cell (space group *Ima*2) with lattice parameters $a = 16.709(3)$ Å, $b = 5.522(3)$ Å, and $c = 5.331(3)$ Å, although very weak peaks corresponding to some impurities such as SrO_2 (pointed out in Figure 2), usually observed when an oxidant agent is used, also appear. The EDS analysis also suggests a majority phase with a composition in agreement with the nominal one. The oxygen content was determined by thermogravimetric analysis. This value was found to be 5.00(5) per unit formula, by reducing the sample according to the following process (Figure 3): $2Sr_2CuGaO_5 \rightarrow Sr_3Ga_2O_6 + SrO + Cu$, and confirmed by X-ray diffraction of the residual products. Such a composition is in agreement with the expected one for a brownmillerite phase and involves the presence of Cu as Cu^{III}.

SAED patterns along [001], [010], and [01$\bar{1}$] zone axes (Figure 4) are in agreement with a brownmillerite structure. However, SAED patterns along [100], [0$\bar{2}$1], and [0$\bar{2}$3] zone axes (Figure 5) indicate a more complex situation, since two kinds of diffraction spots appear: (i) intense, in agreement with the basic brownmillerite unit cell, and (ii) weak, suggesting the presence of a 2-fold superstructure.

The [100] zone axis shows weak reflections at (0 $^1/_2$ 0) and equivalent positions, suggesting that the *b* parameter must be double. The [0$\bar{2}$1] and [0$\bar{2}$3] zone axes exhibit continuous streaks along *a** in alternating

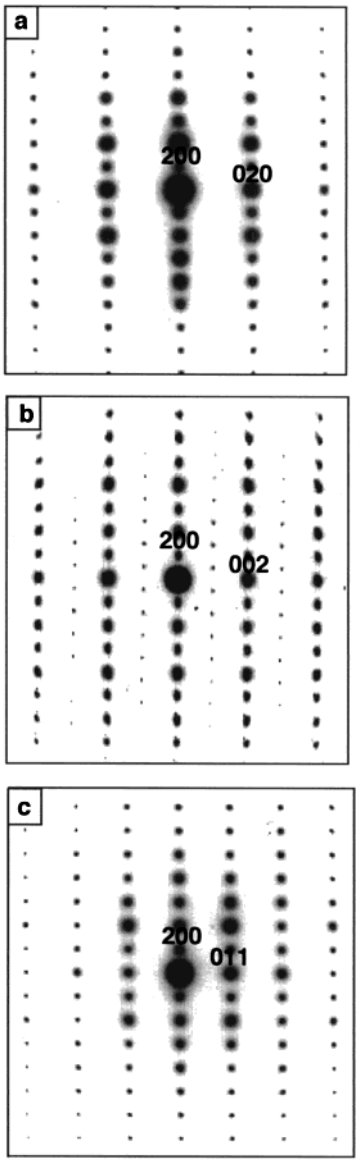

Figure 4. SAED patterns along (a) [001], (b) [010], and (c) [01$\bar{1}$] zone axes.

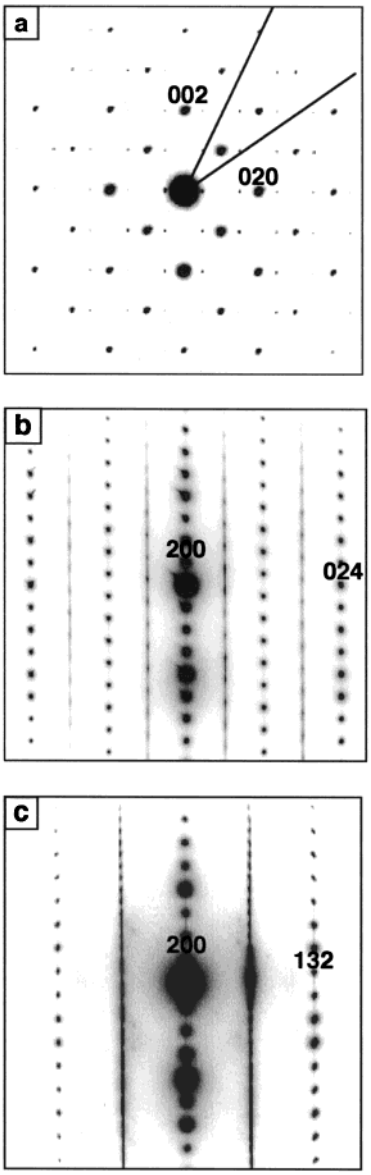

Figure 5. SAED patterns along (a) [100], (b) [0$\bar{2}$1], and (c) [0$\bar{2}$3] zone axes.

rows between the brownmillerite main reflections. Besides, these main reflections show weak diffuse streaking along a^*, suggesting disorder along such a direction. On the other hand, the extra rows can be deduced from the weaker spots observed along [100] (see Figure 5a), which, in fact, correspond to the intersection of the rows in [0$\bar{2}$1] and [0$\bar{2}$3] with the (100) reciprocal plane, as schematically arrowed in Figure 5a.

Figure 6 corresponds to the HREM image along the [01$\bar{1}$] zone axis. This micrograph is characteristic of an ordered brownmillerite material. Indeed, good agreement between experimental and calculated images, taking into account the above model, can be observed in Figure 6b.

Images along [100], [0$\bar{2}$1], and [0$\bar{2}$3] are very helpful to explain the superstructure spots, as well as the expected disorder due to the streaking. The image along [100] (Figure 7) reveals a double *b* periodicity, i.e., 10.8 Å, accounting for the superspots at (0 $^1/_2$ 0) in the SAED pattern. Random changes in contrast along [001], not easily attributable to thickness variations, are probably related to compositional changes leading to an incommensurable modulation along *c*. In this sense, the compositional analysis over small areas, around 60 Å, indicated that the Cu:Ga ratio remains almost unchanged, whereas the Sr content varies from 1.81 to 2.

The image along [0$\bar{2}$1] (Figure 8) shows bright dots with a spacing of 4.8 Å along the [012] direction, i.e., twice the periodicity which should correspond to the basic structure, in agreement with the alternate rows observed in the SAED pattern. Although the distance between bright fringes, along the perpendicular direction, is 8.4 Å, as expected from the basic structure, dots running along this direction are not placed on a straight line, but shifted with respect to the others by $^1/_4$ along [012]. The displacements, however, do not happen in an ordered way, leading to cumulative displacements with a random arrangement, giving rise to disorder along *a*, in agreement with the streaking observed in the diffraction pattern (Figure 5b). A similar situation was found along the [0$\bar{2}$3] zone axis (Figure 9). In this case, bright dots spaced 3.1 Å must be, again, attributed to

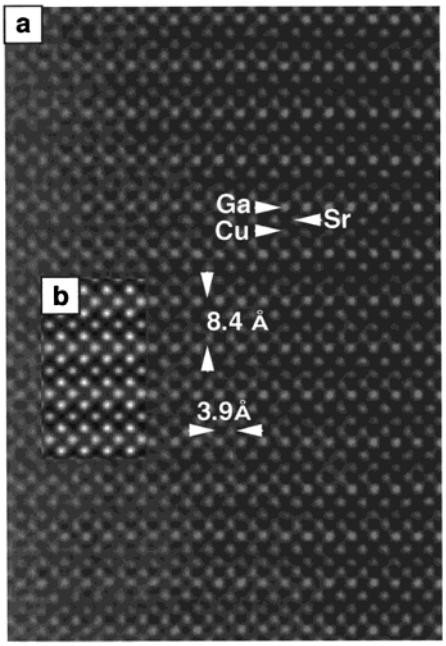

Figure 6. (a) HREM micrograph along the [0$\bar{1}$1] direction and (b) the corresponding calculated image.

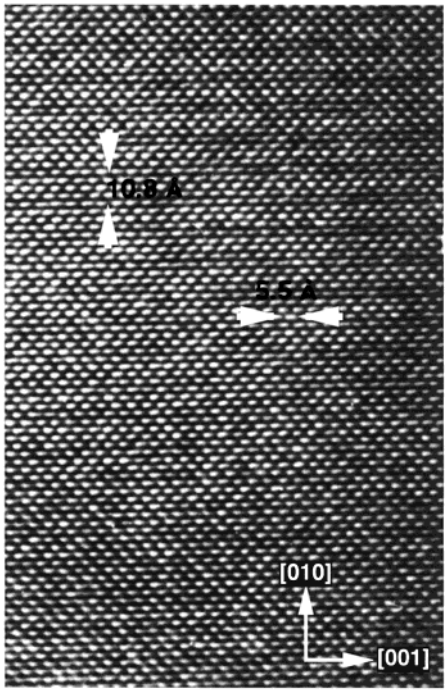

Figure 7. HREM image along the [100] direction.

the superstructure because the expected periodicity was 1.5 Å.

According to the above results, Sr_2CuGaO_5 must present a related brownmillerite structure. In fact, SAED patterns and HREM images corresponding to [001] and [01$\bar{1}$] zone axes are in agreement with this unit cell. However, structural information along [100], [0$\bar{2}$1], and [0$\bar{2}$3] zone axes indicates a double unit cell along the *b* direction.

Similar order−disorder phenomena have been observed on several compounds containing Ga and Co tetrahedrally coordinated[12] as well as on the higher terms (n = 3 and 4) of the homologous series $GaSr_2Ca_{n-1}Cu_nGaO_{2n+3}$.[6,7] Such phenomena have been attributed to the presence of two kinds of tetrahedral chains along the *c* axis while the basic brownmillerite structure is preserved, with Ga at tetrahedral positions and Cu at octahedral ones. However, the superstructure could also be due to a different arrangement of oxygen vacancies, since Ga can also adopt an octahedral coordination[11,13] while lower oxygen environments, such as pyramidal, square planar, or linear, are also possible for Cu[14] in related compounds.

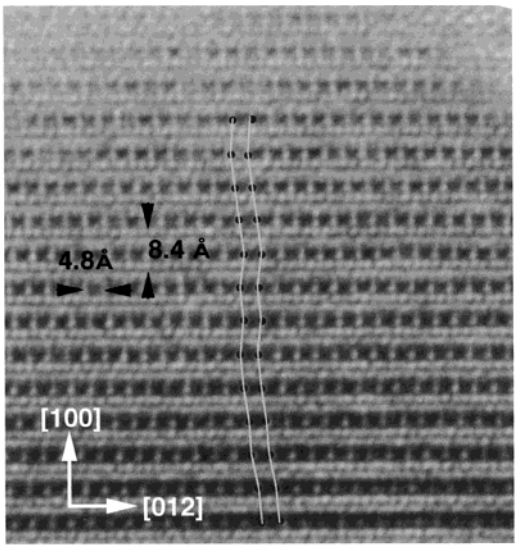

Figure 8. HREM image along the [0$\bar{2}$1] direction. Disorder along *a* is marked.

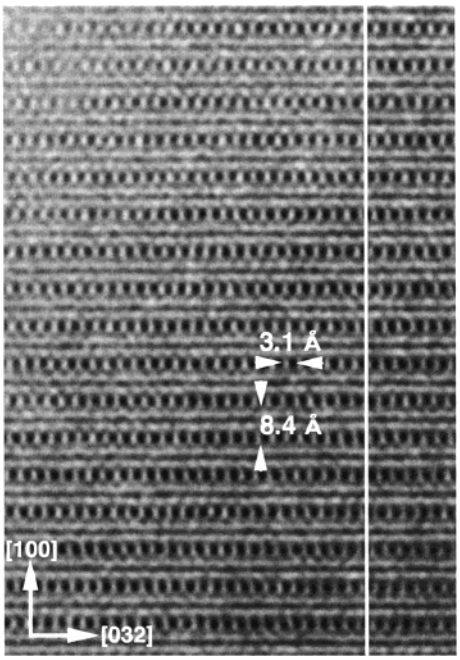

Figure 9. HREM image along the [0$\bar{2}$3] direction. Disorder along *a* is clearly appreciated.

(12) Krekels, T.; Milat, O.; Van Tendeloo, G.; Amelinckx, S.; Babu, T. G. N.; Wright, A. J.; Greaves, C. *J. Solid State Chem.* **1993**, *105*, 313.
(13) Marezio, M.; Remeika, J. P.; Dernier, P. D. *Inorg. Chem.* **1968**, *7* (7), 1337.
(14) Ohshima, E.; Kikuchi, M.; Izumi, F.; Hiraga, K.; Oku, T.; Nakajima, S.; Ohnishi, N.; Morri, Y.; Funahashi, S.; Syono, Y. *Physica C* **1994**, *221*, 261.

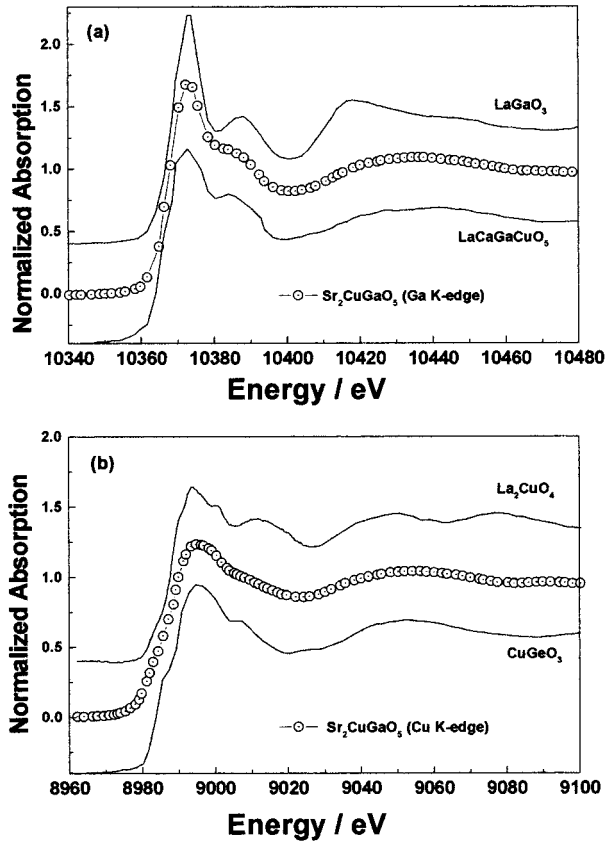

Figure 10. Normalized XANES spectra corresponding to the sample and the reference compounds: (a) Ga K-edge and (b) Cu K-edge.

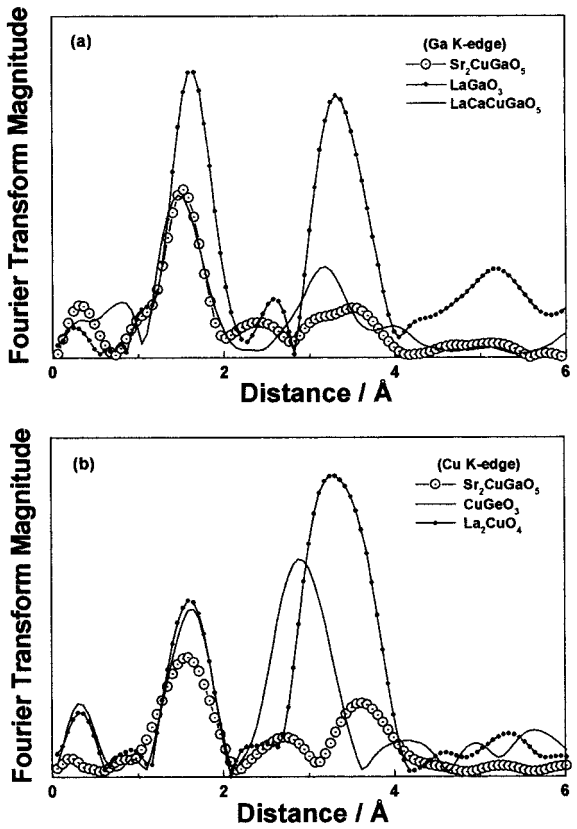

Figure 11. Fourier transform magnitude corresponding to the EXAFS signals characteristic of the sample and reference compounds: (a) Ga K-edge and (b) Cu K-edge.

On the basis of the above information, it seems necessary to gather information about the cation coordination. In this sense, two different types of information can be obtained by using the same experimental X-ray absorption spectroscopy (XAS) setup: The X-ray absorption near edge structure (XANES) is related to the oxidation state and to the stereochemical coordination of the absorbing atoms, and the extended X-ray absorption fine structure (EXAFS) gives the radial distribution function around these atoms.

XAS experiments were performed at the Ga and Cu K-edges. To study the Ga environment, two possible atomic environments, such as tetrahedral and octahedral, should be considered. For that purpose, $LaGaO_3$ and $LaCaGaCuO_5$ were used as a reference for Ga octahedrally and tetrahedrally coordinated, respectively. Figure 10a shows the Ga K-edge XANES spectra corresponding to those references and Sr_2CuGaO_5, which is very similar to $LaCaGaCuO_5$, where Ga ions present a tetrahedral environment. This fact suggests that Ga ion shows tetrahedral coordination in Sr_2CuGaO_5.

The Cu K-edge XANES spectrum of the Sr_2CuGaO_5 sample is shown in Figure 10b. For comparison purposes, the spectra of two references, La_2CuO_4 and $CuGeO_3$, with an octahedral Cu environment have been plotted. The former compound is built up of $Cu-O_6$ octahedra that present $Cu-O_4^{basal}$ distances of 1.89 Å, $Cu-O_2^{apical}$ distances of 2.41 Å, and $O^{basal}-Cu-O^{apical}$ and $O^{basal}-Cu-O^{basal}$ angles equal to 90° at room temperature.[15] Nevertheless, $CuGeO_3$ is built up by more distorted octahedra with $Cu-O_4^{basal}$ distances of 1.93 Å and $Cu-O_2^{apical}$ distances of 2.75 Å, and more important, the $Cu-O^{apical}$ bond is not perpendicular to the basal plane, giving an $O^{basal}-Cu-O^{apical}$ angle equal to 95.66° at room temperature.[16] That different octahedral Cu environment makes it possible for the two features at 9044 and 9070 eV in La_2CuO_4 to become only one broad band at 9050 eV in $CuGeO_3$. Under this assumption and by comparison of the references and XANES spectra, it can be assumed that Cu presents an octahedral environment in Sr_2CuGaO_5 with a very distorted coordination octahedron, where the $Cu-O^{apical}$ bonds are not perpendicular to the basal plane. This highly distorted structure can be understood taking into account that the Sr_2CuGaO_5 compound is not stable under ambient conditions, the application of high pressure being necessary.

Additionally, EXAFS[17] experiments were performed on these compounds. The magnitudes of the Fourier transform (FT) are shown in Figure 11. To fit the EXAFS signals, the backscattering functions were calculated[18] and then the S_0^2 factor was obtained by fitting the reference compounds.

In Figure 11a, the first peaks (centered at 1.5 or 1.6 Å) are related to Ga−O distances. The EXAFS results for the $LaGaO_3$ reference are given in Table 1. It should

(15) Cava, R. J.; Santoro, A.; Jonson, D. W., Jr.; Rodees, W. W. *Phys. Rev. B* **1987**, *35*, 6716.

(16) Braden, M.; Wilkendorf, G.; Lorenzana, J.; Ain, M.; McIntyre, G. J.; Behruzi, M.; Heger, G.; Dhalenne, G.; Revcolevschi, A. *Phys. Rev. B* **1996**, *54*, 1105.

(17) See for instance: Koningsberger, D. C.; Prins, R. *X-ray Absorption Principles Applications, Techniques of EXAFS, SEXAFS and XANES*; Wiley: New York, 1988; p 3.

(18) Rehr, J. J.; Zabinsky, S. I.; Albers, R. C. *Phys. Rev. Lett.* **1992**, *69*, 3397.

Table 1. EXAFS Parameters of the References and $SrCuGaO_5$ Sample at the Ga and Cu K-Edges[a]

sample	pair	R (Å)	N (crystal)	NS_0^2 (fit)	σ (Å)	S_0^2
$LaGaO_3$ (octa-Ga)	Ga−O1	1.951*	2*	1.6	0.05	0.8
	Ga−O2	2.031*	2*	1.6	0.05	0.8
	Ga−O3	2.007*	2*	1.6	0.05	0.8
$LaCaCuGaO_5$ (tetra-Ga)	Ga−O2	1.795*	2*	2.0	0.07	1.0
	Ga−O3	1.89*	1*	1.0	0.06	1.0
	Ga−O3	1.90*	1*	1.0	0.06	1.0
Sr_2CuGaO_5 (sample)	Ga−O1	1.80	2	2.0	0.07	
	Ga−O2	1.90	2	2.0	0.07	
La_2CuO_4	Cu−O1	1.89*	4*	3.5	0.06	0.875
	Cu−O2	2.41*	2*			
$CuGeO_3$	Cu−O1	1.93*	4*	3.5	0.06	0.875
	Cu−O2	2.755*	2*			
Sr_2CuGaO_5 (sample)	Cu−O1	1.92	3.8	3.3	0.07	
	Cu−O2					

[a] Values marked with an asterisk have been taken from the reported crystallographic data. R stands for the distance; N is the number of neighbors; σ correspond to the Debye−Waller factor; S_0^2 is the inelastic losses factor. EXAFS expression for a Gaussian distribution of N_j atoms at mean distances R_j around the absorbing atom: $\chi(k) = S_0^2\sum_j(N_j/kR_j^2)e^{-2k^2\sigma_j^2}e^{(-\Gamma_jR_j/k)}f_j(k)\sin[2kR_j + \phi_j(k)]$. $\phi_j(k) = 2\delta(k) + \gamma_j(k)$ ≡ phase shift ($\delta(k)$ and $\gamma_j(k)$ being the central and backscattering atom phase shifts). $f_j(k)$ ≡ magnitude of the backscattering amplitude of the jth neighbor atom. k/Γ_j ≡ convolution of the mean free path of the photoelectron traveling from the absorbing atom to the backscatterer in the jth shell and the lifetime of the core hole.

be noted that values of N (number of neighbors) and S_0^2 (inelastic loss factor)[18] could not be fitted separately because they appear as a product in the EXAFS expression.[17] The fit of the reference compounds permits the S_0^2 factor to be obtained for a particular environment. To obtain the N value in the crystal, it should be assumed that S_0^2 does not change from samples having the same atomic environment. A second Ga−O reference has been measured, $LaCaCuGaO_5$, which presents GaO_4 tetrahedral coordination with the three different distances given in Table 1. By proceeding as in the octahedral reference, a similar, but not equal, S_0^2 factor has been obtained for the tetrahedral coordination.

Before performing the fit of the Ga environment for Sr_2CuGaO_5, one can compare the FT magnitudes given in Figure 11a. Peaks near 1.5 Å are related to the first coordination sphere (formed by Ga−O distances). It is clear that, in agreement with XANES spectra, Sr_2CuGaO_5 presents a considerable similarity with the tetrahedral $LaCaGaCuO_5$ reference, which has a smaller number of neighbors and shorter distances than the octahedral $LaGaO_3$. Taking into account that XANES spectroscopy indicates a tetrahedral coordination, EXAFS data should be analyzed by considering the backscattering and the inelastic loss factor to be the same as for the $LaCaCuGaO_5$. The fitting parameters are gathered in Table 1. From these parameters, it seems clear that the Sr_2CuGaO_5 sample has GaO_4 tetrahedra formed by two different Ga−O distances of 1.80 and 1.90 Å.

A similar procedure has been followed to analyze the Cu environment EXAFS data. We have used $CuGeO_3$ and La_2CuO_4 as reference compounds. It should be noted that the corresponding FT magnitude for $CuGeO_3$ (Figure 11b) presents a peak near 1.6 Å that corresponds to the four basal distances at 1.93 Å. It is not possible to observe the two apical Cu−O distances (at 2.755 Å) because they are superimposed to the next Cu−Ge neighbors. The La_2CuO_4 case is similar because, at room temperature, there is not enough signal to have a clear peak. In both cases the peak appearing at 1.6 Å is only related to the CuO_4 coordination given by the basal plane of the octahedra, and from EXAFS data, it is not possible to evaluate the larger $Cu-O^{apical}$ octahedron

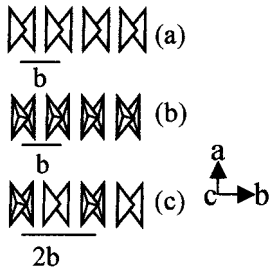

Figure 12. Schematic representation of three possible arrangements of tetrahedral chains along the [001] direction.

distances. Under these circumstances, only the short Cu−O distances appearing in the CuO_6 octahedra can be determined in the Sr_2CuGaO_5 sample; values are given in Table 1. EXAFS analysis reinforces the conclusion that the Ga environment is tetrahedral and Cu coordination is octahedral, although heavily distorted.

The ensemble of results support the stabilization of the $n = 1$ term with a brownmillerite-related structure but involving additional order along b and disorder along a. Such an ordering along b can be induced by changing the orientation of the tetrahedral chains—tilting 180° around a. Parts a and b, respectively, of Figure 12 show the two kinds of tetrahedral chains viewed along the [001] direction. If these chains alternate in an ordered way along the [010] axis, a 2-fold brownmillerite superstructure along b is obtained, as indicated in Figure 12c. In this structure, tetrahedral chains are related by a displacement vector of $^1/_2$ [111], as schematically shown in Figure 13a. A similar shift could be expected when the two kinds of tetrahedral chains are present, i.e., a displacement vector of $^1/_4$ [221]—considering the described superstructure along b—as shown in Figure 13b. Indeed, in Figures 8 and 9, displacements of the periodicity of about $^1/_4$ in the perpendicular direction to a are observed every 8.4 Å or half a brownmillerite unit cell, but they are randomly arranged. This can be better understood in Figure 14, where random displacements of the tetrahedral chains have been represented, from right to left along a with respect to the layer immediately below, giving rise to cumulative translations.

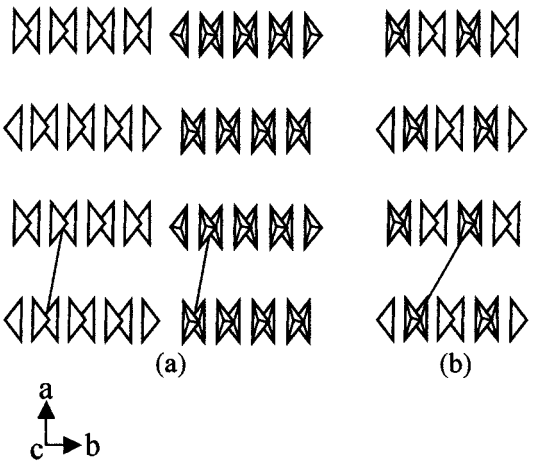

Figure 13. Schematic representation of the tetrahedral stacking layer along *a* in (a) brownmillerite, $4a_c \times a_c\sqrt{2} \times a_c\sqrt{2}$, and (b) the brownmillerite superstructure, $4a_c \times 2a_c\sqrt{2} \times a_c\sqrt{2}$.

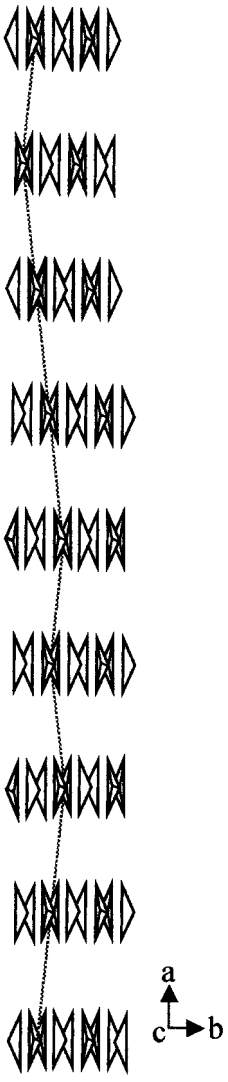

Figure 14. Hypothetical schematic representation showing disorder in the stacking of the tetrahedral layers along the *a* direction.

The proposed model not only explains the superstructure along *b* and disorder along *a*, but also the fact that the superstructure is only observed along certain directions, which are effectively those where tetrahedral rotation can be detected, as along [0$\bar{2}$1] and [0$\bar{2}$3] but not along [01$\bar{1}$] and/or [010], where the contrast produced by the two kinds of chains is the same. In the case of the [100] zone axis, although the two kinds of tetrahedral chains can be theoretically distinguished, it is worth mentioning that since they alternate along *a* with octahedral layers, the different contrast produced by the two kinds of chains is combined with the contrast produced by octahedral layers, which must be prevalent. However, the double periodicity along *b* is observed. At this point, it is worth recalling that XAS experiments suggest a highly distorted CuO_6 octahedral environment. Such a distortion could lead to slight copper displacements from its ideal position, giving rise to a double *b* parameter. Along *a*, the distorted Cu layers must be compensated by the intermediate Ga tetrahedral layers. These two effects would be added to the above description of the tetrahedral chains, enhancing the contrast observed along the [100] zone axis.

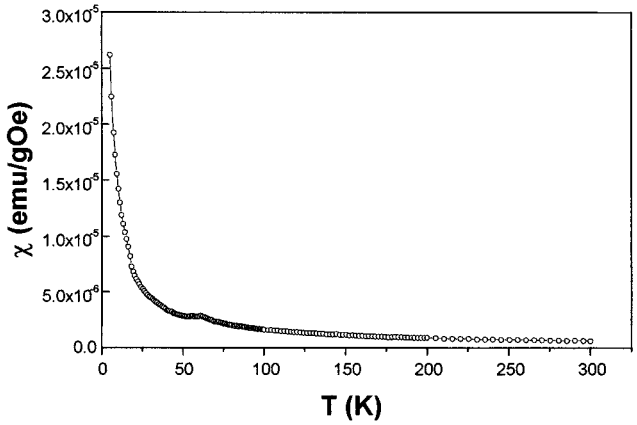

Figure 15. Magnetic susceptibility vs temperature for Sr_2CuGaO_5.

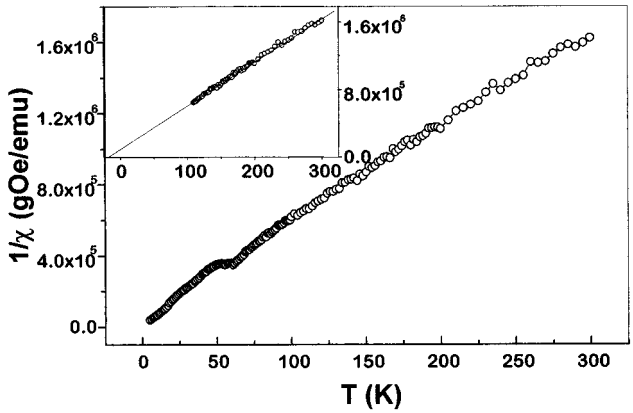

Figure 16. $1/\chi$ vs T for Sr_2CuGaO_5. The inset shows the Θ value.

Finally, susceptibility measurements indicate a paramagnetic behavior (Figure 15) as could be expected due to the loss of 2D CuO_2 planes. On the other hand, the calculated moment in the paramagnetic region (150−300 K), taking into account the Curie−Weiss law, is 2.5 μB, close to the theoretical one, 2.83 μB, if only Cu^{III} is considered to exist. This result is consistent with the oxygen content determined by thermogravimetric analysis (TGA). The anomaly observed around 60 K is more clearly seen when $1/\chi$ is plotted vs T (Figure 16). This could be related to a small antiferromagnetic component

since the Curie temperature, $\Theta = -19$ K, obtained by from the $1/\chi$ plot, is negative, as observed in the inset of Figure 16. Such a behavior could be related to a structural transition involving the distortion of $[CuO_6]$ octahedra.

Concluding Remarks

The $n = 1$ term of the $GaSr_2Ca_{n-1}CunO_{2n+3}$ homologous series of superconducting materials, with a Sr_2CuGaO_5 composition, has been stabilized. High-pressure synthesis together with an oxidizing agent was needed to stabilize Cu^{III}. A brownmillerite-related superstructure is proposed for this new material. Doubling of the *b* parameter is suggested from the microstructural study, probably due to an ordered alternation of two kinds of tetrahedral chains, related by a 180° tilt. The superstructure is, then, only detected along directions in which rotation of the tetrahedral chains can be distinguished, such as [100], $[0\bar{2}1]$, and $[0\bar{3}2]$. The stacking of these layers along *a* does not happen in an ordered way, but involves random displacements, leading to disorder along this direction. An XAS study reinforces the structural analysis suggesting Cu in octahedral coordination and Ga in tetrahedral sites.

Acknowledgment. We acknowledge the staffs in charge of the DCI storage ring of LURE for beam time allocation; special thanks are given to Dr. A. Traverse for experimental assistance. Financial support through Research Project MAT98-0648 (CICYT, Spain) is gratefully acknowledged. We are also grateful to Profs. M. Takano (Kyoto University), O. Terasaki (Tohoku University), and K. Hiraga (Tohoku University) for helpful discussions.

CM0111884